MATHEMATICAL ENGINEERING
TECHNICAL REPORTS

Feedback Control through Networks with Packet Loss: Mixed H_2/H_∞ Approach and Application to a Teleoperating System

Ornwadee RATANAPINUNCHAI, Hideaki ISHII, and
Shinji HARA

(Communicated by Kazuo Murota)

METR 2007–32 May 2007

DEPARTMENT OF MATHEMATICAL INFORMATICS
GRADUATE SCHOOL OF INFORMATION SCIENCE AND TECHNOLOGY
THE UNIVERSITY OF TOKYO
BUNKYO-KU, TOKYO 113-8656, JAPAN

WWW page: http://www.i.u-tokyo.ac.jp/mi/mi-e.htm

Feedback Control through Networks with Packet Loss: Mixed H_2/H_∞ Approach and Application to a Teleoperating System

Ornwadee RATANAPINUNCHAI*, Hideaki ISHII†, and Shinji HARA*

May 16, 2007

Abstract

We consider a networked control system that utilizes unreliable channels where packets may be lost. Assuming that such losses can be modeled as stochastic processes, we propose a mixed H_2/H_∞ control approach for controller synthesis. The designed controller exploits the information regarding the losses and is hence called mode dependant. The approach is applied to a bilateral teleoperating system. In the numerical results, the proposed control shows desired performance in the achievable norms and time responses.

Keywords: Multiobjective control, Networked control, Random packet losses, Stochastic H_∞ and H_2 control, Teleoperating system.

1 Introduction

A networked control system is a system whose control loop is closed via a communication channel. While such a structure provides the benefits of using wired/wireless networks, the limitation on channel bandwidth may cause problems for its control. When the bandwidth is not sufficient for transmitting control related signals, data delay or loss can occur. This in turn degrades the performance of the overall system and can even cause

---

*Department of Information Physics and Computing, Graduate School of Information Science and Technology, The University of Tokyo, 7-3-1, Hongo, Bunkyo-ku Tokyo 113-8656, Japan. E-mail: {Ornwadee_Ratanapinunchai, Shinji_Hara}@ipc.i.u-tokyo.ac.jp.

†Department of Computational Intelligence and Systems Science, Tokyo Institute of Technology, 4259-J2-54, Nagatsuta-cho, Midori-ku, Yokohama 226-8502, Japan. E-mail: ishii@dis.titech.ac.jp.

This work was supported in part by the Ministry of Education, Culture, Sports, Science and Technology, Japan, under Grant No. 17760344 and Japan Science and Technology Agency under the CREST program.

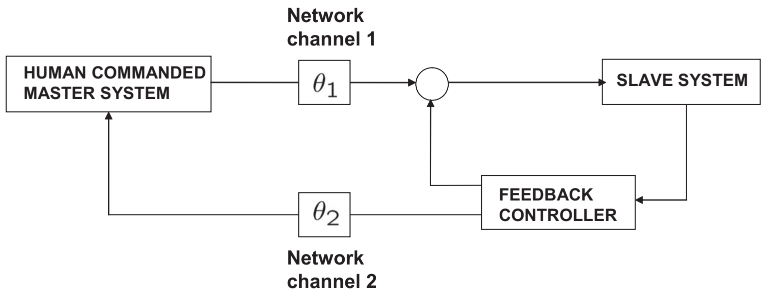

Figure 1: Bilateral teleoperating system

instability. There has been a growing interest in the control community towards dealing with communication limitations in networked control.

In this paper, we focus on the unreliability in the communication and in particular the issue of packet loss. The objective is two fold. In the first part, we model networked control systems via the jump system approach and then develop a controller design method under the criterion of the stochastic H_2 and H_∞ norms. In the second part, the control design is applied to a teleoperating system.

First, we model control systems with lossy channels in a general setting. We assume that all packet losses in the system are stochastic processes and that their loss probabilities are known a priori. We follow the approach of stochastic jump systems, which has been employed in the literature; see, e.g., [8, 9, 18, 19]. The controller to be designed is mode dependant in that it takes account of the information regarding the losses at each moment. The proposed design is a stochastic version of the mixed H_2/H_∞ control that has been recognized to be useful for linear time-invariant (LTI) systems (e.g., [15]) and Markovian jump systems [5]. Our result is for output feedback control and is based on the H_∞ design of [18]. It provides a condition in the form of linear matrix inequalities (LMIs).

In the second part, we apply the design method to a bilateral teleoperating system. Fig. 1 shows a simple setup of such a system. It is a dual robot system having a master robot operated by a human and a slave robot that is remotely located and tracks the master's movement communicated over a channel. In the reverse direction, the environmental force exerted on the slave is also transmitted over the channel to be reflected back to the master. This force reflection enables the human operator to adjust the motion and to enhance his/her task performance. For a survey on this subject, we refer to [7].

In the bilateral control of teleoperation, the passivity-based approach initiated by [1] has been widely used. One characteristic is that stability can be achieved under arbitrary time delay in the communication. Under this approach, several works deal with delays and data losses including [2, 6, 16] employing a passive interpolation method and [13] using a model-based control design.

On the other hand, there is a line of research based on H_∞ control that considers the worst-case performance. This was first studied in [12]. Its basic feature is to model delay in the communication channel as system uncertainty and to utilize H_∞ control and μ-synthesis techniques. Compared to the passivity approach, there are three advantages: (i) The system performance can be considered at the design stage. (ii) The performance under both situations when the slave robot is and is not in contact with environmental objects can be guaranteed. (iii) It does not require passivity of the master/slave nor that of the operator/environment models. Other works following this approach include [3, 11, 14, 20].

Here, the design procedure follows that of [12]. The channels are modeled by the packet loss processes as mentioned above. In contrast to many existing results, we model the teleoperating system in the discrete-time domain. We assume that delays are constant; delays that are time-varying and stochastic may also be modeled in the framework with necessary modification. Numerical results exhibit that the controller designed under the scheme is advantageous over deterministic ones not taking account of the loss. This is shown through results on achievable norms as well as time responses.

This paper is organized as follows: Section 2 provides preliminary results on the stochastic systems considered here. In Section 3, we formulate the mixed H_2/H_∞ control design problem and present the main result. In Section 4, the scheme is applied to a teleoperating system. We conclude the paper in Section 5.

2 Preliminaries

In this paper, we model a discrete-time system with stochastic packet loss in the communication channel by a stochastic jump system. In this section, we provide some preliminary material on such systems.

Consider the system with the state-space realization as

$$\mathcal{P}_\theta : \begin{bmatrix} x(k+1) \\ z(k) \end{bmatrix} = \begin{bmatrix} \mathcal{A}_{\theta(k)} & \mathcal{B}_{\theta(k)} \\ \mathcal{C}_{\theta(k)} & \mathcal{D}_{\theta(k)} \end{bmatrix} \begin{bmatrix} x(k) \\ w(k) \end{bmatrix}, \tag{1}$$

where $x(k) \in \mathbb{R}^{n_x}$ is the state, $w(k) \in \mathbb{R}^{n_w}$ is the input, and $z(k) \in \mathbb{R}^{n_z}$ is the output. The mode $\theta(k)$ of the system is an i.i.d. stochastic process and takes values in a finite set $\mathcal{N} := \{1, \dots, N\}$; the probability for the value $i \in \mathcal{N}$ to occur is given by $p_i = \Pr\{\theta(k) = i\}$ for all k with $p_i \in [0,1]$ and $\sum_{i=1}^{N} p_i = 1$. For simplicity, we assume that $p_i > 0$ for each $i \in \mathcal{N}$. This system can be viewed as a Markovian jump system for which there are results available in, e.g., [4, 10].

We introduce the notation used in the paper. We deal with a sequence $x := \{x(k)\}_{k=0}^{\infty}$ which depends on a mode sequence $\Theta = \{\theta(k)\}_{k=0}^{\infty}$. The space of square summable (stochastic) signals is defined by $\ell_2^n := \{\{x(k)\}_{k=0}^{\infty} : x(k) \in \mathbb{R}^n,\ k = 0, 1, \ldots,$ is a random variable depending on Θ_k and $\|x\|_2 < \infty\}$, where $\Theta_k := \{\theta(0), \ldots, \theta(k)\}$ and the ℓ_2-norm is defined by $\|x\|_2^2 := \sum_{k=0}^{\infty} E_{\Theta_{k-1}}[x(k)^T x(k)]$.

2.1 Mean-square stability analysis

The form of stability used with the jump system in (1) is in the mean-square sense as defined next.

Definition 2.1 The system $\mathcal{P}_\theta$ in (1) with $w(\cdot) \equiv 0$ is *mean-square stable (MSS)* if for every initial state $x(0)$,

$$\lim_{k\to\infty} E_{\Theta_{k-1}}[\|x(k)\|^2] = 0.$$

There is a necessary and sufficient condition to check for MSS as stated below (e.g., [4, 10]).

Lemma 2.1 The system $\mathcal{P}_\theta$ in (1) is mean-square stable if and only if there exists a matrix $G > 0$ such that

$$\sum_{i=1}^{N} p_i \mathcal{A}_i^T G \mathcal{A}_i - G < 0.$$

2.2 H_∞ norm analysis

The following definition is the stochastic version of the H_∞ norm for discrete-time jump linear systems [4, 17].

Definition 2.2 Assume that the system $\mathcal{P}_\theta$ in (1) is mean-square stable and let $x(0) = 0$. Then, its H_∞ norm is given by

$$\|\mathcal{P}_\theta\|_\infty := \sup_{w \in \ell_2^{nw},\ w \neq 0} \frac{\|z\|_2}{\|w\|_2}.$$

We now move toward the analysis of the H_∞ performance of the system. It requires the following definition of controllability for the jump system.

Definition 2.3 The system $\mathcal{P}_\theta$ in (1) is *weakly controllable* if for every initial state x_0 and every final state x_f, there exists a finite time T_c and an input w_c such that $\Pr[x(T_c) = x_f \mid x(0) = x_0] > 0$.

The following is the bounded real lemma due to [17].

Lemma 2.2 Assume that $\mathcal{P}_\theta$ is weakly controllable. The system $\mathcal{P}_\theta$ is mean-square stable and $\|\mathcal{P}_\theta\|_\infty < \gamma$ if and only if there exists a matrix $G > 0$ that satisfies

$$\sum_{i=1}^{N} p_i \begin{bmatrix} \mathcal{A}_i & \mathcal{B}_i \\ \mathcal{C}_i & \mathcal{D}_i \end{bmatrix}^T \begin{bmatrix} G & 0 \\ 0 & I_{n_z} \end{bmatrix} \begin{bmatrix} \mathcal{A}_i & \mathcal{B}_i \\ \mathcal{C}_i & \mathcal{D}_i \end{bmatrix} - \begin{bmatrix} G & 0 \\ 0 & \gamma^2 I_{n_w} \end{bmatrix} < 0. \tag{2}$$

The weak controllability assumption in the result ensures that the disturbance can affect the system state. If the system is not weakly controllable, the condition in (2) is still sufficient, but may not be necessary [17]. We note that a synthesis result based on the lemma above is presented in [18], which is employed in the next section.

2.3 H_2 norm analysis

Consider the system in (1). We now introduce the definition of the H_2 norm [4].

Definition 2.4 Assume that the system $\mathcal{P}_\theta$ in (1) is mean-square stable and let $x(0) = 0$. Then, its H_2 norm is given by

$$\|\mathcal{P}_\theta\|_2^2 := \sum_{s=1}^{n_w} \|z_s\|_2^2,$$

where z_s is the output $(z(0), z(1), \ldots)$ of $\mathcal{P}_\theta$ when the impulse signal $w = (w(0), w(1), \ldots) = (e_s, 0, \ldots)$ is applied, and $e_s \in \mathbb{R}^{n_w}$ is formed by one at the sth entry and zero elsewhere for $s = 1, \ldots, n_w$.

As in the deterministic case, the H_2 norm can be expressed by the observability Gramian. The proposition below gives an analysis condition for the H_2 performance.

Proposition 2.1 The system $\mathcal{P}_\theta$ in (1) is mean-square stable and $\|\mathcal{P}_\theta\|_2 < \nu$ if and only if there exist matrices $G > 0$ and Q satisfying

$$\begin{aligned} &\sum_{i=1}^{N} p_i \mathcal{A}_i^T G \mathcal{A}_i + \sum_{i=1}^{N} p_i \mathcal{C}_i^T \mathcal{C}_i - G < 0, \\ &\sum_{i=1}^{N} p_i (\mathcal{B}_i^T G \mathcal{B}_i + \mathcal{D}_i^T \mathcal{D}_i) - Q < 0, \\ &\mathrm{Tr}(Q) < \nu^2. \end{aligned} \tag{3}$$

The proof of the proposition is given in the Appendix. This is a slight modification of a result in [4]. The key characteristic lies in the inequalities in (3) having the same form as those in Lemmas 2.1 and 2.2. This aspect will become important in the synthesis.

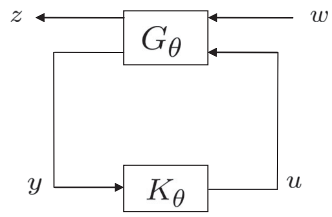

Figure 2: Closed-loop system

3 Mixed H_2/H_∞ controller synthesis

In this section, we present a mixed H_2/H_∞ approach for jump linear systems. We develop a design procedure for a dynamic output feedback controller such that under random modes the closed-loop is mean-square stable and achieves desired performance in both H_2 and H_∞ norms.

3.1 Problem formulation

Consider the closed-loop system shown in Fig. 2. The generalized plant G_θ has the realization given by

$$\begin{bmatrix} x(k+1) \\ z(k) \\ y(k) \end{bmatrix} = \begin{bmatrix} A_{\theta(k)} & B_{w,\theta(k)} & B_{\theta(k)} \\ C_{z,\theta(k)} & D_{zw,\theta(k)} & D_{z,\theta(k)} \\ C_{\theta(k)} & D_{w,\theta(k)} & 0 \end{bmatrix} \begin{bmatrix} x(k) \\ w(k) \\ u(k) \end{bmatrix},$$

where $x(k) \in \mathbb{R}^{n_x}$ is the state, $w(k) \in \mathbb{R}^{n_w}$ is the disturbance, $z(k) \in \mathbb{R}^{n_z}$ is the controlled output, $u(k) \in \mathbb{R}^{n_u}$ is the control input, and $y(k) \in \mathbb{R}^{n_y}$ is the measurement. The signal $\theta(k) \in \mathcal{N}$ denotes the mode of the system; as in the previous section, it is an i.i.d. stochastic process with $p_i = \Pr\{\theta(k) = i\} > 0$ for any k, i, and $\sum_{i=1}^{N} p_i = 1$.

The controller K_θ has the state-space form as

$$\begin{bmatrix} \hat{x}(k+1) \\ u(k) \end{bmatrix} = \begin{bmatrix} \hat{A}_{\theta(k)} & \hat{B}_{\theta(k)} \\ \hat{C}_{\theta(k)} & \hat{D}_{\theta(k)} \end{bmatrix} \begin{bmatrix} \hat{x}(k) \\ y(k) \end{bmatrix}, \tag{4}$$

where $\hat{x}(k) \in \mathbb{R}^{n_c}$ is the controller state. The controller is time-varying and can switch between the N modes depending on the current jump parameter $\theta(k)$. We use the term *mode dependant* controller to refer to its dependency on $\theta(k)$.

With this structure of the generalized plant and the controller, the closed-loop system, denoted by $\mathcal{P}_\theta$, can be written in the form of (1) with

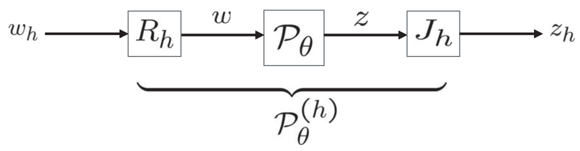

Figure 3: Multi-channel system

the system matrices as

$$
\begin{aligned}
\mathcal{A}_{\theta(k)} &= \begin{bmatrix} A_{\theta(k)} + B_{\theta(k)}\hat{D}_{\theta(k)}C_{\theta(k)} & B_{\theta(k)}\hat{C}_{\theta(k)} \\ \hat{B}_{\theta(k)}C_{\theta(k)} & \hat{A}_{\theta(k)} \end{bmatrix}, \\
\mathcal{B}_{\theta(k)} &= \begin{bmatrix} B_{w,\theta(k)} + B_{\theta(k)}\hat{D}_{\theta(k)}D_{w,\theta(k)} \\ \hat{B}_{\theta(k)}D_{w,\theta(k)} \end{bmatrix}, \\
\mathcal{C}_{\theta(k)} &= \begin{bmatrix} C_{z,\theta(k)} + D_{z,\theta(k)}\hat{D}_{\theta(k)}D_{w,\theta(k)} & D_{w,\theta(k)}\hat{C}_{\theta(k)} \end{bmatrix}, \\
\mathcal{D}_{\theta(k)} &= D_{zw,\theta(k)} + D_{z,\theta(k)}\hat{D}_{\theta(k)}D_{w,\theta(k)}.
\end{aligned}
\tag{5}
$$

Next, we discuss the method of measuring the performance of the closed-loop system by viewing it as a multi-channel system. This method is based on the multiobjective control for LTI systems in [15]. Consider the system depicted in Fig. 3, where h is the parameter that determines the norm criterion applied to the system $\mathcal{P}_\theta^{(h)}$ from w_h to z_h. In particular, the system $\mathcal{P}_\theta^{(2)}$ is for the H_2 norm and $\mathcal{P}_\theta^{(\infty)}$ is for the H_∞ norm. The matrices J_h and R_h select the appropriate input/output channels and are composed of 0 and 1 entries.

The mixed H_2/H_∞ control problem can be stated as follows: Consider the system in Fig. 2. Given $\gamma > 0$, find a mean-square stabilizing mode-dependant controller K_θ that minimizes $\|\mathcal{P}_\theta^{(2)}\|_2$ subject to $\|\mathcal{P}_\theta^{(\infty)}\|_\infty < \gamma$.

It is noted that we can similarly formulate a problem where the minimization is with respect to the H_∞ norm under a constraint on the H_2 norm. The final result for such a problem can be obtained along the same lines.

3.2 Mixed H_2/H_∞ synthesis: Result

Now, we are ready to state the main result on the mixed H_2/H_∞ controller synthesis, which is given in terms of LMIs. The derivation of this condition can be found in the Appendix.

Theorem 3.1 If there exist matrices $Y = Y^T \in \mathbb{R}^{n_x \times n_x}$ $X = X^T \in \mathbb{R}^{n_x \times n_x}$, $M_i \in \mathbb{R}^{n_u \times n_y}$, $F_i \in \mathbb{R}^{n_u \times n_x}$, $L_i \in \mathbb{R}^{n_x \times n_y}$, and $W_i \in \mathbb{R}^{n_x \times n_x}$ such that

$$\begin{bmatrix} \begin{bmatrix} Y & I & 0 \\ I & X & 0 \\ 0 & 0 & \gamma^2 I \end{bmatrix} & (\bullet)^T & \cdots & (\bullet)^T \\ S_1 & \begin{bmatrix} Y & I & 0 \\ I & X & 0 \\ 0 & 0 & I \end{bmatrix} & \cdots & (\bullet)^T \\ \vdots & \vdots & \ddots & \vdots \\ S_N & 0 & \cdots & \begin{bmatrix} Y & I & 0 \\ I & X & 0 \\ 0 & 0 & I \end{bmatrix} \end{bmatrix} > 0 \tag{6}$$

and

$$\begin{aligned} &\begin{bmatrix} \begin{bmatrix} Y & I \\ I & X \end{bmatrix} & (\bullet)^T & \cdots & (\bullet)^T \\ U_1 & \begin{bmatrix} Y & I & 0 \\ I & X & 0 \\ 0 & 0 & I \end{bmatrix} & \cdots & (\bullet)^T \\ \vdots & \vdots & \ddots & \vdots \\ U_N & 0 & \cdots & \begin{bmatrix} Y & I & 0 \\ I & X & 0 \\ 0 & 0 & I \end{bmatrix} \end{bmatrix} > 0, \\ &\begin{bmatrix} Q & (\bullet)^T & \cdots & (\bullet)^T \\ V_1 & \begin{bmatrix} Y & I & 0 \\ I & X & 0 \\ 0 & 0 & I \end{bmatrix} & \cdots & (\bullet)^T \\ \vdots & \vdots & \ddots & \vdots \\ V_N & 0 & \cdots & \begin{bmatrix} Y & I & 0 \\ I & X & 0 \\ 0 & 0 & I \end{bmatrix} \end{bmatrix} > 0, \\ &\mathrm{Tr}(Q) < \nu^2, \end{aligned} \tag{7}$$

where

$$\begin{aligned} S_i &:= \sqrt{p_i} \begin{bmatrix} YA_i + L_i C_i & W_i & (YB_{w,i} + L_i D_{w,i})R_\infty \\ A_i + B_i M_i C_i & A_i X + B_i F_i & (B_{w,i} + B_i M_i D_{w,i})R_\infty \\ J_\infty(C_{z,i} + D_{z,i} M_i C_i) & J_\infty(C_{z,i} X + D_{z,i} F_i) & J_\infty(D_{zw,i} + D_{z,i} M_i D_{w,i})R_\infty \end{bmatrix}, \\ U_i &:= \sqrt{p_i} \begin{bmatrix} YA_i + L_i C_i & W_i \\ A_i + B_i M_i C_i & A_i X + B_i F_i \\ J_2(C_{z,i} + D_{z,i} M_i C_i) & J_2(C_{z,i} X + D_{z,i} F_i) \end{bmatrix}, \\ V_i &:= \sqrt{p_i} \begin{bmatrix} (YB_{w,i} + L_i D_{w,i})R_2 \\ (B_{w,i} + B_i M_i D_{w,i})R_2 \\ J_2(D_{zw,i} + D_{z,i} M_i D_{w,i})R_2 \end{bmatrix}, \quad i \in \{1, \ldots, N\}, \end{aligned}$$

then there exists a mode-dependant controller K_θ such that the closed-loop system is mean-square stable with $\|\mathcal{P}_\theta^{(2)}\|_2 < \nu$ and $\|\mathcal{P}_\theta^{(\infty)}\|_\infty < \gamma$.

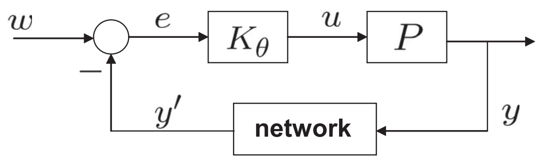

Figure 4: Feedback system with packet loss

The solution to the LMI condition in Theorem 3.1 can be used to construct the system matrices for the controller K_θ in (4) as follows:

$$\begin{aligned}
\hat{D}_i &= M_i,\\
\hat{C}_i &= (F_i - M_iC_iX)(Y^{-1} - X)^{-1},\\
\hat{B}_i &= Y^{-1}L_i - B_iM_i,\\
\hat{A}_i &= -Y^{-1}[Y(A_i - B_iM_iC_i)X + YB_iF_i + L_iC_iX - W_i](Y^{-1} - X)^{-1}.
\end{aligned}$$

It is noted that Theorem 3.1 provides only a sufficient condition for the existence of a controller. This is due to the fact that the closed-loop objectives are guaranteed based on a common Lyapunov function. Thus, the multiple specifications are achieved at the expense of conservatism. However, we remark that the inequality in (6) alone is a necessary and sufficient condition for the H_∞ performance synthesis with $\|\mathcal{P}_\theta^{(\infty)}\|_\infty < \gamma$. Similarly, the inequalities (7) are equivalent to the H_2 synthesis for $\|\mathcal{P}_\theta^{(2)}\|_2 < \nu$.

3.3 Numerical example

We illustrate the effectiveness of the proposed synthesis result through an example. In particular, we show the benefit of using an H_2/H_∞ controller over an H_∞ controller [18]; both are mode dependant.

The system setup is given in Fig. 4, where the plant is an unstable second-order system with poles at 0.5 and 1.1. The network is modeled by a packet loss process $\theta(k) \in \{0, 1\}$, where $\theta(k) = 0$ if the data is lost at time k and $\theta(k) = 1$ if it is received. The loss probability is denoted by $\alpha := \text{Prob}\{\theta(k) = 0\}$. Further, in the network, we employ a *last packet* method specified by

$$y'(k) = \begin{cases} y(k) & \text{if } \theta(k) = 1,\\ y'(k-1) & \text{otherwise.}\end{cases}$$

H_∞ control is used on the complementary sensitivity function T_{yw} and H_2 control on the sensitivity function T_{ew}. Let γ be $\|T_{yw}\|_\infty$ and let ν be $\|T_{ew}\|_2$. Under this setup, there is a trade-off in performance of the two norms. That is, a larger H_∞ norm constraint will allow a smaller H_2 norm

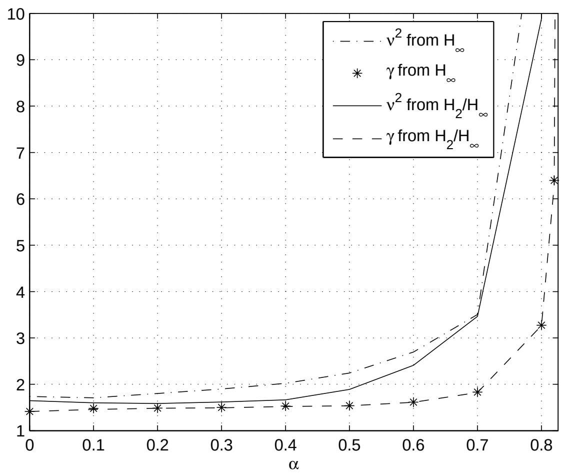

Figure 5: Norms using the H_2/H_∞ controller and the H_∞ controller versus the loss probability α

and vice versa. Fig. 5 shows that the H_2/H_∞ controller outperforms the H_∞ one in the achievable H_2 norm since they have approximately the same H_∞ norms.

4 Application to a teleoperating system

In this section, we study the application of the design approach in the previous section to a bilateral teleoperating system. First, we describe the system setup and formulate the problem. Second, the outline of the design procedure is given. Finally, we provide numerical results and present the accomplished performance from several aspects. We note that the design is performed under only the H_∞ norm criterion; this is due to issues in numerical computation.

4.1 Problem setup

Consider the bilateral teleoperating system in Fig. 6. The systems and signals in the block diagram are as follows:

P_m: Master robot	M_s: Slave system
$K_{f,\theta}$: Feedback controller	θ_1,θ_2: Channels
v_m: Master velocity	v_s: Slave velocity
f_h: Human command force	f_s: Environmental force

Here, the output v_m of the master robot is sent to the slave system as a command input via the channel 1 represented by θ_1, while the feedback

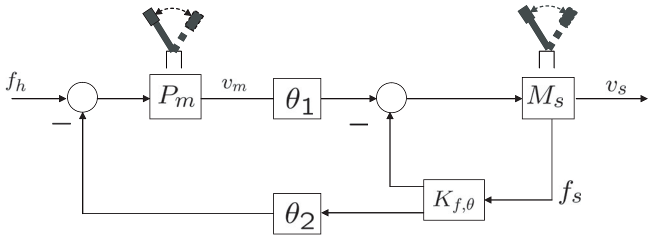

Figure 6: Bilateral teleoperating system (The slave system M_s is in Fig. 7)

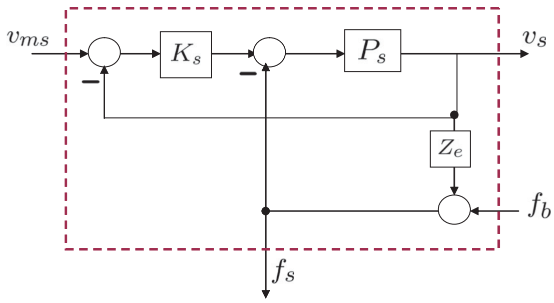

Figure 7: Slave system M_s

control signal is sent back to the master through the channel 2 given by θ_2. The channels are lossy in the sense that $\theta_i(k) \in \{0,1\}$ with the loss probability specified by $\alpha_i = \Pr\{\theta_i(k) = 0\}$ for $i = 1,2$. The slave system M_s in Fig. 6 has a detailed composition shown in Fig. 7, where P_s represents the slave robot, K_{s,θ_1} is the slave local controller, and Z_e is the environmental impedance. The signal f_b is the sensor noise added to regularize the problem.

The slave robot is said to be in *free motion* when it is not in contact with the environment, i.e., when $Z_e = 0$. An important feature of this setup is that when the slave is in free motion, $K_{f,\theta}$ outputs zero, and hence no force is fed back to the master side. On the other hand, the system is in *constrained motion* when the slave system and the environment are in contact.

The slave controller K_{s,θ_1} depends on θ_1 while the feedback controller $K_{f,\theta}$ utilizes both θ_1 and θ_2. This is realized by assuming that acknowledgement messages are sent from the master side to the feedback controller regarding the arrival of packets through the channel 2.

The objective here is to design two mode-dependant controllers, the slave controller K_{s,θ_1} and the feedback controller $K_{f,\theta}$, such that the overall system is stable and desired H_∞ performance is achieved under packet loss in the channels.

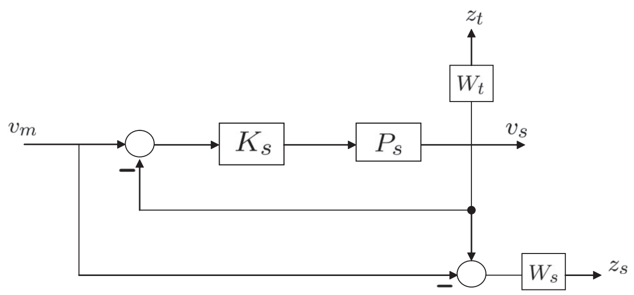

Figure 8: Design of K_s for the classic model and model 1

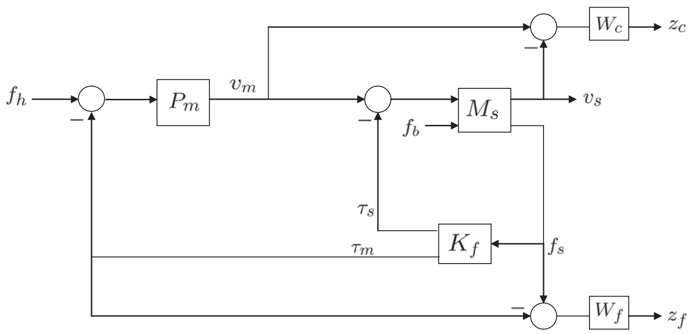

Figure 9: Design of K_f for the classic model

4.2 Design procedure

The outline of the design procedure is as follows. The first step is to design the slave controller and then in the second step, the feedback controller is constructed.

In our study, we design three sets of controllers and compare their performances. (i) Under the *classic model*, no packet loss is assumed. Both controllers are designed using the standard H_∞ synthesis method and do not depend on the loss. The notations K_s and K_f are adopted. (ii) *Model 1* uses the same slave controller as in the classic model, but the feedback controller $K_{f,\theta}$ is mode dependant and is designed by the stochastic H_∞ synthesis method. (iii) The third case is *model 2* where both the slave and feedback controllers K_{s,θ_1} and $K_{f,\theta}$ are mode dependant, and their construction is done via the stochastic H_∞ method.

For each case of controller synthesis, we perform a mixed sensitivity type design under the stochastic H_∞ norm criterion. We briefly introduce the system setups used for synthesis. For the classic model, the slave controller K_s is designed according to Fig. 8 to reduce the tracking error $v_m - v_s$ after suitable weighting. Next, the feedback controller K_f is designed using the

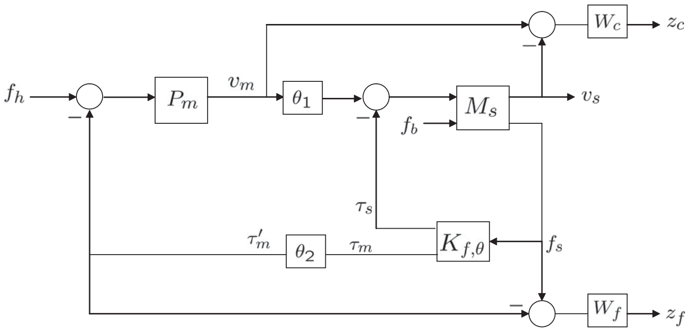

Figure 10: Design of $K_{f,\theta}$ for models 1 and 2

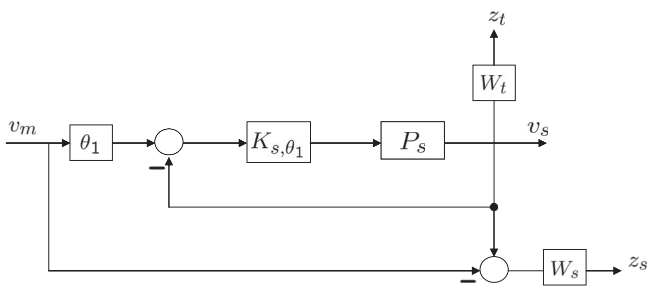

Figure 11: Design of K_{s,θ_1} for model 2

setup in Fig. 9; the objective is to simultaneously minimize $v_m - v_s$ and $f_s - \tau_m$, where τ_m is an output of K_f.

For model 1, the local controller K_s is designed as in the classic model case. In the design of the feedback controller $K_{f,\theta}$, however, the setup in Fig. 10 is used to incorporate the packet loss in the two channels (θ_1, θ_2). The resulting controller has four modes.

In the case of model 2, K_{s,θ_1} is first designed by taking account of the presence of channel 1 through the system shown in Fig. 11. As a result, K_{s,θ_1} depends on θ_1 and has two modes. Once this is accomplished, we construct the feedback controller $K_{f,\theta}$ as in the model 1 case.

4.3 Simulation results

We now present the results obtained through simulations. The parameters used here are mainly due to [11] and are as follows: The master plant P_m and the slave plant P_s are given by discretizing the continuous-time systems P_{mc} and P_{sc}, respectively, with the sampling period $T_s = 1$ msec:

$$P_{mc}(s) = \frac{803.5}{s + 23.6}, \quad P_{sc}(s) = \frac{704.6}{s + 30.6}.$$

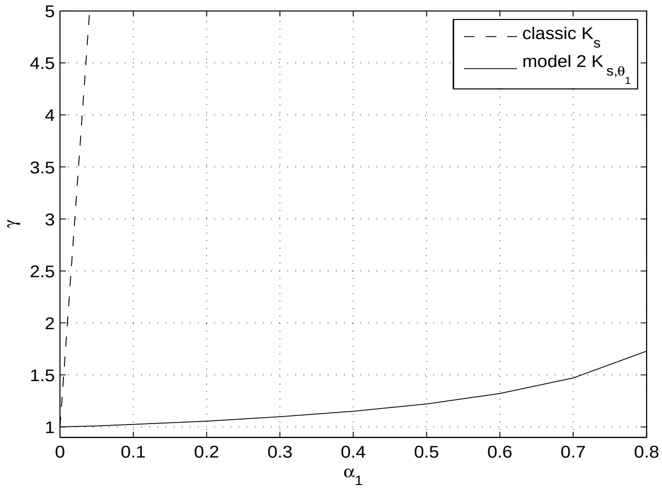

Figure 12: Norms versus the loss probability α_1 for the free motion: Classic model K_s (dashed) and model 2 K_{s,θ_1} (solid)

Similarly, the environment Z_e is obtained by discretizing $Z_{ec}(s) = 74/s$. The weighting functions are chosen similar to those in [11, 12], but are modified.

4.3.1 Norm performance

For the free motion case, Fig. 12 shows the norm comparison with respect to the loss probability α_1 for the classic model with K_s which is independent of the loss and model 2 with a mode-dependant K_{s,θ_1}. The mode-dependant controller exhibits much better performance. Note that since we focus on their tracking ability, the norm is taken only at the weighted tracking error z_s in Fig. 11.

For the constrained motion case, we first examine the norm for the classic model. The norm of the system in Fig. 10 (with the output $z = [z_c^T z_f^T]^T$) is shown by the dash-dot line in Fig. 13. The x-axis represents the loss probability in both channels, which are set to be equal. As expected, the performance quickly degrades as the loss probability increases. Next, we look at the cases with the mode-dependant controllers in Fig. 13. The dashed line represents the result of the model 1 system, and the solid line is for model 2. Clearly, both models perform much better than the classic controller case. Though model 2 seems to perform only slightly better than model 1, the advantage of model 2 will become clear in its time responses.

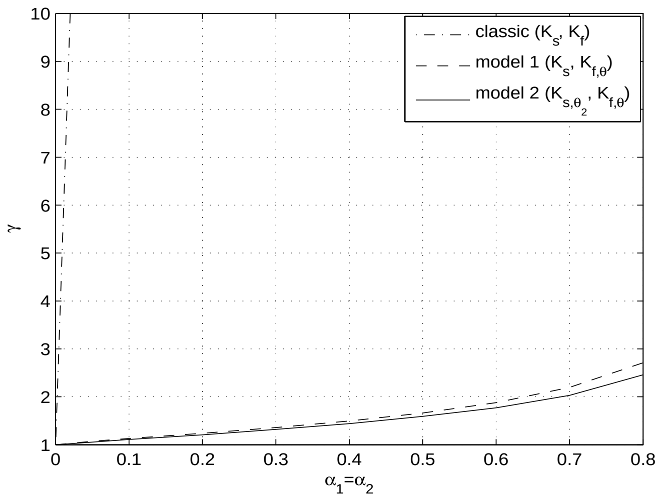

Figure 13: Norms versus the loss probability $\alpha_1 = \alpha_2$ for the constrained motion: Classic model (dash-dot), model 1 (dashed), and model 2 (solid)

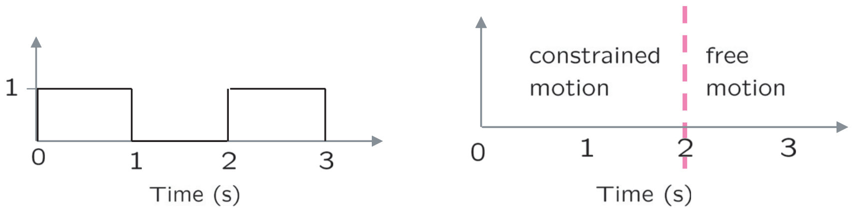

(a) Square wave input

(b) Environment condition

Figure 14: Setup for the time responses

4.3.2 Time responses

In the setup of Fig. 6, the human command force f_h is taken as a square wave signal shown in Fig. 14(a). Regarding the environment, the system is under constrained motion for $0 \leq t \leq 2$, and after $t = 2$, it is under free motion (see Fig. 14(b)). We are interested in the tracking performance of the master-slave system under packet loss. Hence, in Figs. 15, 16, and 17, we plot the time responses of the velocity tracking error $v_m - v_s$ (top plot), the master velocity v_m (middle), and the slave velocity v_s (bottom) for the three models.

The first case is with the classic model under ideal communication, i.e., with $\alpha_1 = \alpha_2 = 0$. The dashed lines in Fig. 15 are the responses. Since the slave is in contact with a spring-like environment at $0 \leq t \leq 2$, the slave velocity v_s is allowed to react only slightly to the change in the command f_h at $t = 0$ and $t = 1$. Due to the tracking design specification, the master velocity v_m is also forced back to zero. Thus, the velocity tracking error

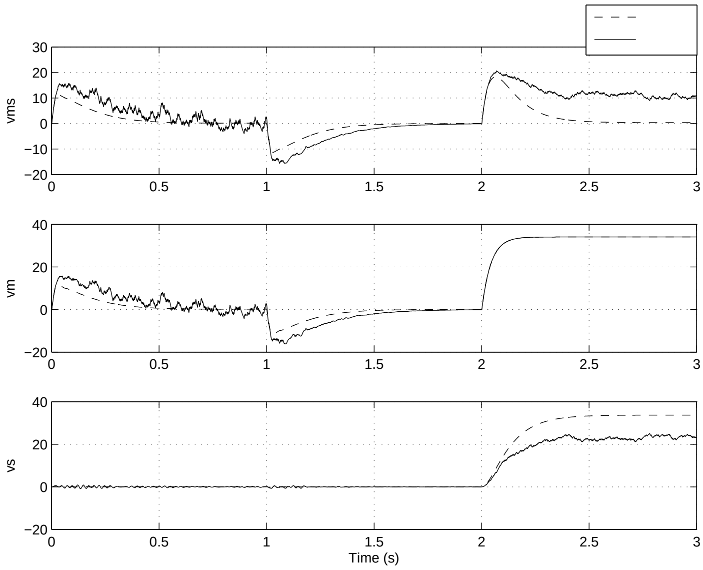

Figure 15: Time responses: The classic model under 30% loss rate (solid) and the classic model under ideal communication (dashed). (Top: $v_m - v_s$, Middle: v_m, Bottom: v_s.)

decays to zero. However, during the free motion at $t \geq 2$, the slave is free to move in compliance with the master. Hence, both v_m and v_s follow the command f_h. The tracking error also slowly goes to zero.

Next, we see how the classic model controller handles packet loss. The solid lines in Fig. 15 are the responses under 30% loss rates in both channels and show that the performance severely degrades. We note that, under the losses, the response is asymmetric about the x-axis. The reason is that when f_h becomes zero, the master is commanded to stay at zero. The feedback controller then needs to reduce its control effort τ_m to zero so that there is no force input to the master. Hence, the loss in channel 1 would help τ_m to decay faster.

The response of the system with model 1 under 30% loss rate in both channels is shown in solid lines in Fig. 16. During the constrained motion, though oscillation still occurs, it can handle losses better than the classic model controller. However, during the free motion, it responds similarly to the classic model since they both use the same mode-independent K_s.

Lastly, we examine the case with model 2 that employs mode-dependant controllers in both the slave and feedback controllers. Its response is shown in solid lines in Fig. 17. It should be noted that both K_{s,θ_1} and $K_{f,\theta}$ are specifically designed to handle 30% loss rate. Not much improvement from model 1 can be seen during the constrained motion; this may be reasonable

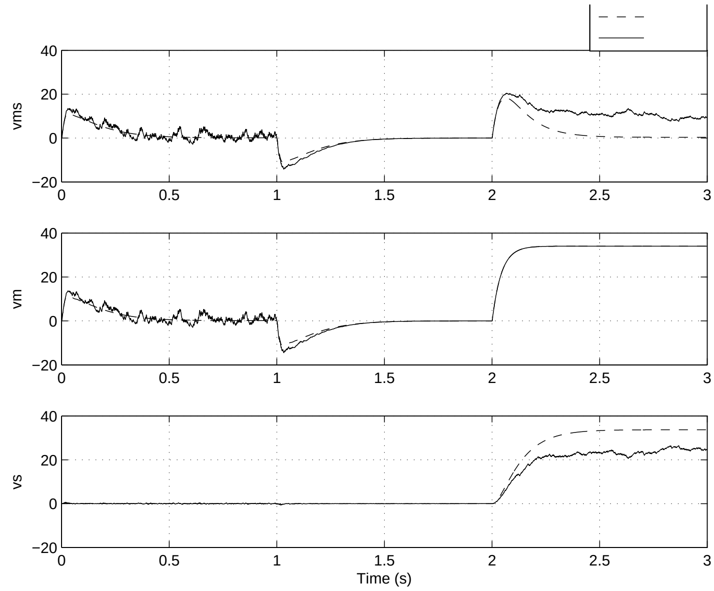

Figure 16: Time response: Model 1 under 30% loss rate (solid) and the classic model under ideal communication (dashed). (Top: $v_m - v_s$, Middle: v_m, Bottom: v_s.)

as the difference in the norms in Fig. 13 was small. However, the advantage of using model 2 is clear in the free motion.

5 Conclusion

In this paper, we focused on the packet loss issue in networked control and proposed a mixed H_2/H_∞ control type design. A detailed study on its application to a bilateral teleoperation was presented. The results show that in both cases of free motion and constrained motion, mode-dependant controllers taking account of the loss information enhance the performance in the achievable norms and time responses. Future research will study the effects of delays and packet losses under time-varying loss rates.

References

[1] R. J. Anderson and M. W. Spong. Bilateral control of teleoperators with time delay. *IEEE Trans. Autom. Control*, 34:494–501, 1989.

[2] P. Berestesky, N. Chopra, and M. W. Spong. Discrete time passivity in bilateral teleoperation over the Internet. In *Proc. IEEE Int. Conf. on Robotics and Automation*, pages 4557–4564, 2004.

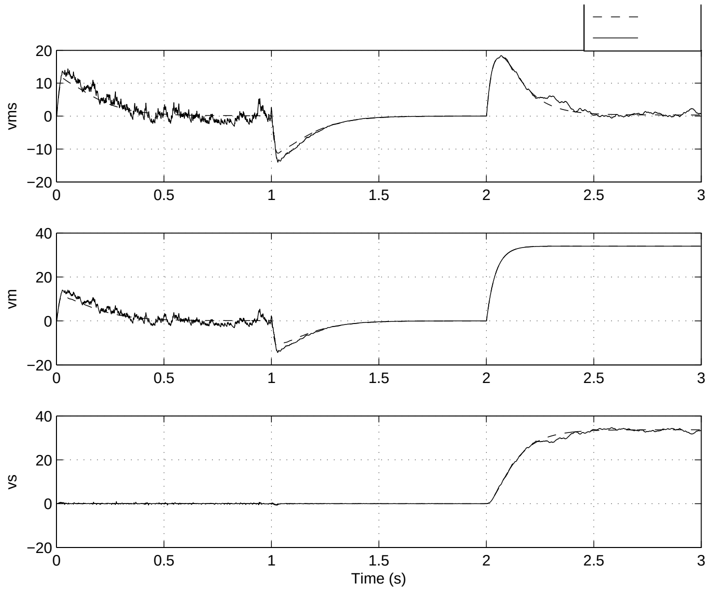

Figure 17: Time response: Model 2 under 30% loss rate (solid) and the classic model under ideal communication (dashed). (Top: $v_m - v_s$, Middle: v_m, Bottom: v_s.)

[3] M. Boukhnifer, A. Ferreira, and J.-G. Fontaine. Scaled teleoperation controller design for micromanipulation over Internet. In *Proc. IEEE Int. Conf. on Robotics and Automation*, pages 4577–4583, 2004.

[4] O. L. V. Costa, M. D. Fragoso, and R. P. Marques. *Discrete-Time Markov Jump Linear Systems*. Springer, London, 2005.

[5] O. L. V. Costa and R. P. Marques. Mixed H^2/H^∞-control of discrete-time Markovian jump linear systems. *IEEE Trans. Autom. Control*, 43:95–100, 1998.

[6] S. Hirche and M. Buss. Packet loss effects in passive telepresence systems. In *Proc. 43rd IEEE Conf. on Decision and Control*, pages 4010–4015, 2004.

[7] P. F. Hokayem and M. W. Spong. Bilateral teleoperation: An historical survey. *Automatica*, 42:2035–2057, 2006.

[8] O. Ç. Imer, S. Yüksel, and T. Başar. Optimal control of LTI systems over unreliable communication links. *Automatica*, 42:1429–1439, 2006.

[9] H. Ishii. H^∞ control with limited communication and message losses. In *Proc. American Control Conf.*, pages 5620–5625, 2006. Also submitted for publication.

[10] Y. Ji, H. J. Chizeck, X. Feng, and K. Loparo. Stability and control of discrete-time jump linear systems. *Control Theory Adv. Technol.*, 7:247–270, 1991.

[11] H.-K. Lee, K. Tanie, and M. J. Chung. Design of a robust bilateral controller for teleoperators with modeling uncertainties. In *Proc. IEEE/RSJ Conf. Intel. Robots & Systems*, pages 1860–1865, 1999.

[12] G. M. H. Leung, B. A. Francis, and J. Apkarian. Bilateral controller for teleoperators with time delay via μ-synthesis. *IEEE Trans. Robotics and Automation*, 11:105–116, 1995.

[13] S. Mastellone, D. Lee, and M. W. Spong. Master-slave synchronization with switching communication through passive model-based control design. In *Proc. American Control Conf.*, pages 3203–3208, 2006.

[14] A. Sano, H. Fujimoto, and M. Tanaka. Gain-scheduled compensation for time delay of bilateral teleoperation systems. In *Proc. IEEE Int. Conf. on Robotics and Automation*, pages 1916–1923, 1998.

[15] C. Scherer, P. Gahinet, and M. Chilali. Multiobjective output-feedback control via LMI optimization. *IEEE Trans. Autom. Control*, 42:896–911, 1997.

[16] C. Secchi, S. Stramigioli, and C. Fantuzzi. Dealing with unreliabilities in digital passive geometric telemanipulation. In *Proc. IEEE/RSJ Int. Conf. on Intelligent Robots and Systems*, pages 2823–2828, 2003.

[17] P. Seiler and R. Sengupta. A bounded real lemma for jump systems. *IEEE Trans. Autom. Control*, 48:1651–1654, 2003.

[18] P. Seiler and R. Sengupta. An H^∞ approach to networked control. *IEEE Trans. Autom. Control*, 50:356–364, 2005.

[19] B. Sinopoli, L. Schenato, M. Franceschetti, K. Poolla, M. I. Jordan, and S. S. Sastry. Kalman filtering with intermittent observations. *IEEE Trans. Autom. Control*, 49:1453–1464, 2004.

[20] J. Yan and S. E. Salcudean. Teleoperation controller design using H^∞-optimization with application to motion-scaling. *IEEE Trans. Control Systems Technology*, 4:244–258, 1996.

Appendix

5.1 Proof of Proposition 2.1

We first note that under the assumption that the system is MSS, a matrix $G > 0$ satisfying the first inequality (3) exists [4]. Now, we evaluate the l_2 norm of the output z_s, $s \in \{1, \ldots, n_w\}$, when the input sequence $(e_s, 0, \ldots)$ is applied as follows:

$$\begin{aligned}
\|z_s\|_2^2 &= \sum_{k=0}^{\infty} E_{\Theta_k} \|z_s(k)\|^2 \\
&= \sum_{k=0}^{\infty} E_{\Theta_k} [\|\mathcal{C}_{\theta(k)} x(k) + \mathcal{D}_{\theta(k)} w(k)\|^2] \\
&= \sum_{k=0}^{\infty} E_{\Theta_{k-1}} [\sum_{i=1}^{N} p_i \|\mathcal{C}_i x(k) + \mathcal{D}_i w(k)\|^2],
\end{aligned}$$

where the last equality holds after evaluating the expectation over $\theta(k)$. Using the first inequality in (3) and also the assumptions on the initial state and the input, we can obtain

$$\begin{aligned}
\|z_s\|_2^2 < \sum_{k=0}^{\infty} \big\{ & E_{\Theta_{k-1}} [x(k)^T G x(k)] - E_{\Theta_k} [x(k)^T \mathcal{A}_{\theta(k)}^T G \mathcal{A}_{\theta(k)} x(k)] \\
& + E_{\Theta_k} [w(k)^T \mathcal{D}_{\theta(k)}^T \mathcal{D}_{\theta(k)} w(k)] \big\}.
\end{aligned}$$

Substituting $x(k+1) - \mathcal{B}_{\theta(k)} w(k)$ into $\mathcal{A}_{\theta(k)} x(k)$ yields

$$\begin{aligned}
\|z_s\|_2^2 < \sum_{k=0}^{\infty} \big\{ & E_{\Theta_{k-1}} [x(k)^T G x(k)] - E_{\Theta_k} [x(k+1)^T G x(k+1)] \\
& + 2 E_{\Theta_k} [x(k+1)^T G \mathcal{B}_{\theta(k)} w(k)] - E_{\Theta_k} [w(k)^T \mathcal{B}_{\theta(k)}^T G \mathcal{B}_{\theta(k)} w(k)] \\
& + E_{\Theta_k} [w(k)^T \mathcal{D}_{\theta(k)}^T \mathcal{D}_{\theta(k)} w(k)] \big\}.
\end{aligned}$$

Next, by cancellation of the first two terms in the summation and by using the initial state and the input, we obtain

$$\begin{aligned}
\|z_s\|_2^2 &< E_{\Theta_0} [2x(1)^T G \mathcal{B}_{\theta(0)} e_s - e_s^T \mathcal{B}_{\theta(0)}^T G \mathcal{B}_{\theta(0)} e_s + e_s^T \mathcal{D}_{\theta(0)}^T \mathcal{D}_{\theta(0)} e_s] \\
&= E_{\Theta_0} [e_s^T \mathcal{B}_{\theta(0)}^T G \mathcal{B}_{\theta(0)} e_s + e_s^T \mathcal{D}_{\theta(0)}^T \mathcal{D}_{\theta(0)} e_s].
\end{aligned}$$

Thus, we have $\|z_s\|_2^2 < \sum_{i=1}^{N} p_i [e_s^T (\mathcal{B}_i^T G \mathcal{B}_i + \mathcal{D}_i^T \mathcal{D}_i) e_s]$. By the norm definition, it follows that

$$\|\mathcal{P}_\theta\|_2^2 = \sum_{s=1}^{n_w} \|z_s\|_2^2 < \mathrm{Tr} \sum_{i=1}^{N} p_i (\mathcal{B}_i^T G \mathcal{B}_i + \mathcal{D}_i^T \mathcal{D}_i). \qquad \square$$

5.2 Proof of Theorem 3.1

The mixed H_2/H_∞ synthesis result can be obtained by following along similar lines as in the case for the H_∞ synthesis in [18]. The outline is as follows:

First, apply the analysis results for the H_∞ norm in Lemma 2.2 and for the H_2 norm in Proposition 2.1 to the closed-loop system whose state-space matrices are given in (5). Here, in the two analysis results, the matrix G is taken to be common.

Then, to obtain equivalent inequalities that are convex in the design parameters, we invoke an approach that has been developed in the context of H_∞ control for LTI systems. In particular, we use the one with a linearizing change of controller variables and a congruence transformation (see, e.g., [15, 18]). As a consequence of the common matrix G, the resulting inequalities in (6) and (7) have common matrices X and Y. $\square$